Proton single-particle strength in ^{19}F measured via the ^{18}O(d,n) reaction

A. Terakawa, H. Orihara, M. Oura, M. Hosaka, H. Suzuki, K. Kumagai, and Y. Kikuchi
Cyclotron and Radioisotope Center, Tohoku University, Sendai 980-8578, Japan

T. Tohei, T. Nakagawa, J. Takamatsu, A. Narita, and K. Hosomi
Department of Physics, Graduate School of Tohoku University, Sendai 980-8578, Japan

K. Ishii
Department of Quantum Science and Energy Engineering, Graduate School of Tohoku University, Sendai 980-8578, Japan

G. C. Jon
Institute of Physics, Academia Sinica, Nankang, Taipei 11592, Taiwan

K. Miura
Department of Physics, Tohoku Institute of Technology, Sendai 982-8577, Japan

H. Ohnuma
Department of Physics, Chiba Institute of Technology, Narashino-shi, Chiba 275-0023, Japan
(Received 7 June 2002; published 13 December 2002)

Proton single-particle strengths in ^{19}F were investigated up to an excitation energy of 14 MeV through the (d,n) reaction on ^{18}O at $E_d=25$ MeV. Spectroscopic strengths were deduced from adiabatic-deuteron-breakup-approximation analysis. Most of the strengths for the $2s1d$-shell orbitals were observed in the present measurement. Strength distributions were compared with the shell-model predictions in the framework of the complete $2s1d$-shell basis. Results for the $1d_{5/2}$ and $2s_{1/2}$ strengths were in good agreement with the shell-model calculation, but the theoretical estimate for the $1d_{3/2}$ strength did not reproduce the observation. The occupation probabilities and single-particle energies of proton orbitals near the Fermi surface for ^{18}O were evaluated from a combined analysis of the present stripping data and previous proton pickup data.

DOI: 10.1103/PhysRevC.66.064313 PACS number(s): 21.10.Pc, 25.45.Hi, 27.20.+n

I. INTRODUCTION

One-nucleon transfer reactions are useful probes to study the single-particle nature of nuclear excitation. The stripping reaction, transferring one nucleon into a single-particle orbital with quantum numbers nlj, allows one to extract the spectroscopic factors which manifest the single-particle feature of the final states in the residual nucleus. Because of the completeness relation of the wave functions, the summation of the spectroscopic factors over all final states with nlj yields the number of holes in the orbital for the initial ground state [1,2]. Furthermore, the distribution of the spectroscopic factors gives us information about not only the single-particle energy but also the spreading width due to the damping of the single-particle excitation.

In recent years experimental efforts to measure occupation probabilities of shell model orbitals have been made to study nucleon-nucleon correlations in nuclei. Occupation numbers of the $3s$ proton in the Pb region have precisely been evaluated using both relative spectroscopic factors and charge density differences between neighboring nuclei [3,4]. The shapes of the proton Fermi surface for the $2s1d$-shell and $1f2p$-shell nuclei have been studied from occupation probabilities and single-particle energies deduced from analyses on the basis of both stripping and pickup reactions on the same target nucleus [5–7].

Proton single-particle states in the $2s1d$-shell nuclei have extensively been investigated by means of high-resolution (d,n) experiments [8,9]. In comparison with a recent shell-model prediction [10], which is based on the complete $2s1d$-shell space, the results for the ^{20,22}Ne$(d,n)^{21,23}$Na reactions [9] have shown that a 25-MeV (d,n) reaction provides reliable spectroscopic factors.

In this paper we present the result for the ^{18}O$(d,n)^{19}$F reaction at 25 MeV. Although proton single-particle strengths in ^{19}F have so far been studied [11–13] using (^{3}He,d) and (α,t) reactions, little is known about the high-lying strengths above the one-proton emission threshold at $E_{\rm exc}=7.994$ MeV. On the other hand, the shell model predicts [10] that the significant strengths of the $1d_{3/2}$ proton reside in the excitation region above $E_{\rm exc}=9$ MeV. In this work we aim to investigate the proton single-particle strength of the $2s1d$-shell orbitals up to $E_{\rm exc}=14$ MeV, and to test the shell-model wave functions [10] by comparing the experimental results with the predictions. Furthermore, we attempt to deduce occupation probabilities and single-particle energies of proton orbitals near the Fermi surface for ^{18}O using the present stripping results in combination with pickup data obtained from the ^{18}O$(d,^3$He$)^{17}$N reaction [14].

II. EXPERIMENTAL PROCEDURE

The experiment was performed using a momentum-analyzed beam of 25-MeV deuterons from the AVF cyclotron

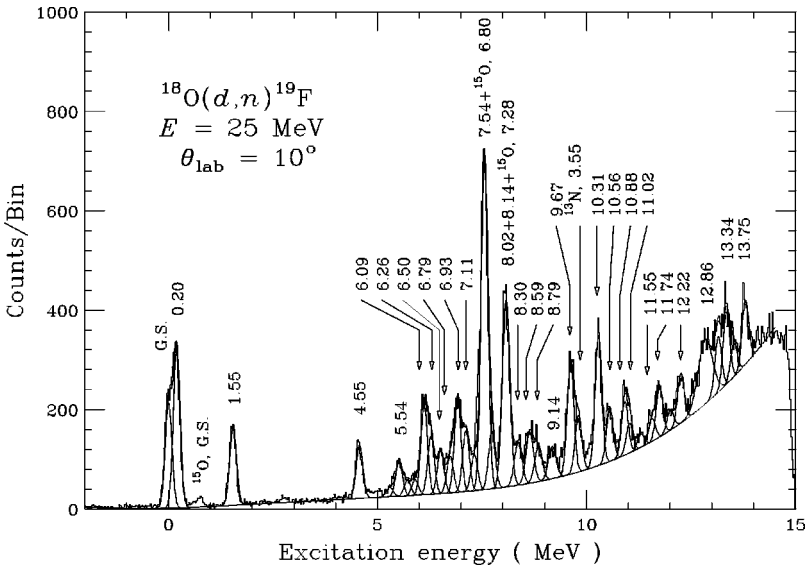

FIG. 1. An excitation-energy spectrum for the ^{18}O$(d,n)^{19}$F reaction at $\theta_{lab}=10°$ and at $E_d=25$ MeV. The histogram is shown in 25-keV wide bins. The solid lines represent the results for the peak-deconvolution analysis.

at the Cyclotron and Radioisotope Center (CYRIC), Tohoku University. The target was ^{18}O gas isotopically enriched to 98.7% and kept in a gas cell with a diameter of 1.5 cm and a length of 2 cm along with the beam direction. The target thickness was 1.5 mg/cm^2. The window of the gas cell was a 10-mg/cm^2 thick platinum foil.

Energies of the emitted neutrons were measured by means of a time-of-flight (TOF) technique using the CYRIC TOF facility [15,16]. Twelve neutron detectors containing liquid organic scintillator NE213 of 23.4 l in total were located at a distance of 43.2 m from the target. Angular distributions of the neutrons were measured with the beam-swinger system in an angular range from $\theta_{lab}=10°$ to 60° in the laboratory system.

For the neutron-gamma discrimination the pulse shape discrimination method was used. In addition, the low energy neutrons overlapping the fast neutrons in the neutron energy spectrum were removed using a software threshold for the light output spectra from the detectors. Finally, the excitation-energy spectra in ^{19}F were obtained from the energy spectrum through the kinematical calculation for the ^{18}O$(d,n)^{19}$F reaction at 25 MeV.

Figure 1 shows the excitation-energy spectrum of the ^{18}O$(d,n)^{19}$F reaction at $\theta_{lab}=10°$, together with the result of a peak-fitting procedure using Gaussian functions with continuous backgrounds. The background in the present experiment includes both experimental and physical background neutrons. The experimental background is due to the windows of the gas cell, while the physical background comes from the reaction processes such as deuteron breakup and neutron evaporation. For the background subtraction in the peak-fitting procedure, the fourth degree polynomial was used to reproduce the overall background shape. The present measurement has covered the excitation region up to $E_{exc}=14$ MeV in ^{19}F. The overall energy resolution of about 180 keV has been achieved for the most energetic neutron.

The neutron-detection efficiency has been determined via an activation analysis for the ^{7}Li$(p,n)^7$Be reaction [15,16]. Errors in the absolute magnitude of the cross section have been estimated to be less than 15%.

III. ANALYSIS

A. Distorted-wave analysis

Zero-range distorted-wave analyses with finite-range and nonlocality corrections were performed using the code DWUCK4 [17] in the framework of adiabatic-deuteron-breakup approximation (ADBA) [18] to assign orbital angular momentum l of the transferred proton, and to deduce spectroscopic factors. An adiabatic-deuteron potential was produced by the Wales and Johnson method [19] using proton and neutron potentials at a half energy of the incident deuteron. These nucleon potentials were taken from the global potential of Becchetti and Greenlees for a proton [20] and that of Martin for a neutron [21]. The parameters for the

TABLE I. Potential parameters used in the present analysis.

[a]		^{18}O+d	^{19}F+n [b]	^{18}O+p
V_{RV}	(MeV)	98.44	$51.7-0.26E$	adj [c]
r_{RV}	(fm)	1.18	1.18	1.25
a_{RV}	(fm)	0.74	0.66	0.65
W_{IV}	(MeV)	-0.40	$-2.9+0.2E$	
r_{IV}	(fm)	1.30	1.28	
a_{IV}	(fm)	0.61	0.55	
W_{IS}	(MeV)	15.45	$9.3-0.15E$	
r_{IS}	(fm)	1.30	1.28	
a_{IS}	(fm)	0.60	0.55	
V_{SO}	(MeV)	5.95	5.7	$\lambda=25$ [d]
r_{SO}	(fm)	1.01	1.00	1.25
a_{SO}	(fm)	0.58	0.41	0.65
r_C	(fm)	1.30		1.25
N_{NL}	(fm)	0.43	0.85	

[a]The potential parameters consist of real-volume (RV), imaginary-volume (IV), imaginary-surface (IS), spin-orbit (SO), and Coulomb (C) terms. Nonlocality correction parameters N_{NL} are also listed. Finite-range parameter N_{FR} was 0.695 fm.

[b]E is the neutron energy in the exit channel.

[c]Well depth is adjusted to reproduce the separation energy.

[d]Thomas spin-orbit strength.

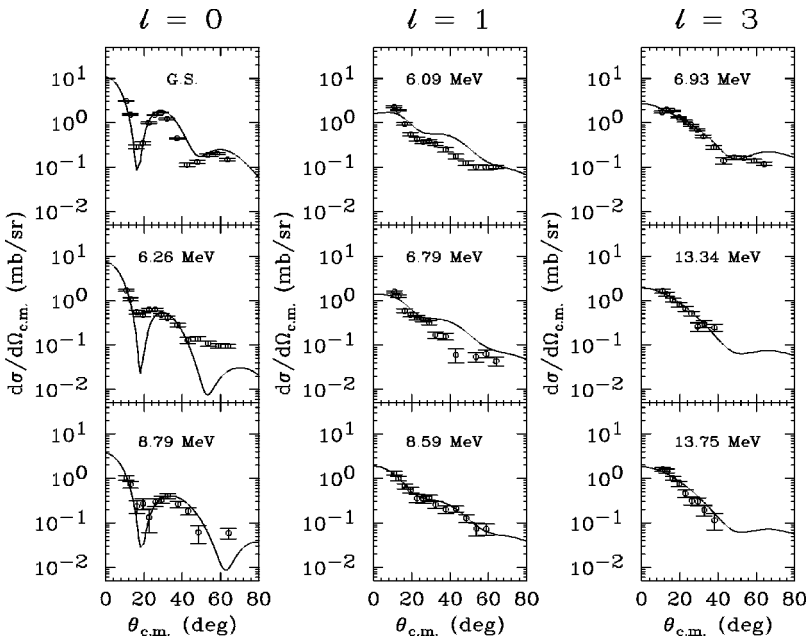

FIG. 2. Differential cross sections for the $l=0$, 1, and 3 transitions measured through the ^{18}O$(d,n)^{19}$F reaction at 25 MeV. The solid lines represent the results for the ADBA calculations.

emitted neutrons were also taken from Ref. [21]. The single-particle wave function of the transferred particle was generated by the separation-energy method with a local Woods-Saxon potential. In the case of proton unbound transitions leading to final states at $E_{\rm exc}>7.994$ MeV, resonant form factors were calculated according to the procedure of Vincent and Fortune [22]. The potential parameters used in the present analysis are listed in Table I.

Spectroscopic factors S_{lj} were obtained from the following relation for the spin zero target:

$$\left(\frac{d\sigma}{d\Omega}\right)_{\rm exp}=1.55(2J+1)C^2S_{lj}\left(\frac{d\sigma}{d\Omega}\right)_{\rm calc}, \qquad (1)$$

where C is a Clebsh-Gordan coefficient. The normalization factor of 1.55 is a standard value [17] for a (d,n) reaction.

Measured angular distributions of the differential cross sections are shown in Figs. 2 and 3, together with the results of the ADBA analysis. The measured angular distributions are well reproduced by the theoretical results, as far as the data at the forward angles are concerned. In the present analysis, l assignments have been made for 28 transitions up to $E_{\rm exc}=14$ MeV.

B. Shell-model calculation

Microscopic description of the low-lying levels in the mass region $A=17-39$ can be made in terms of the shell

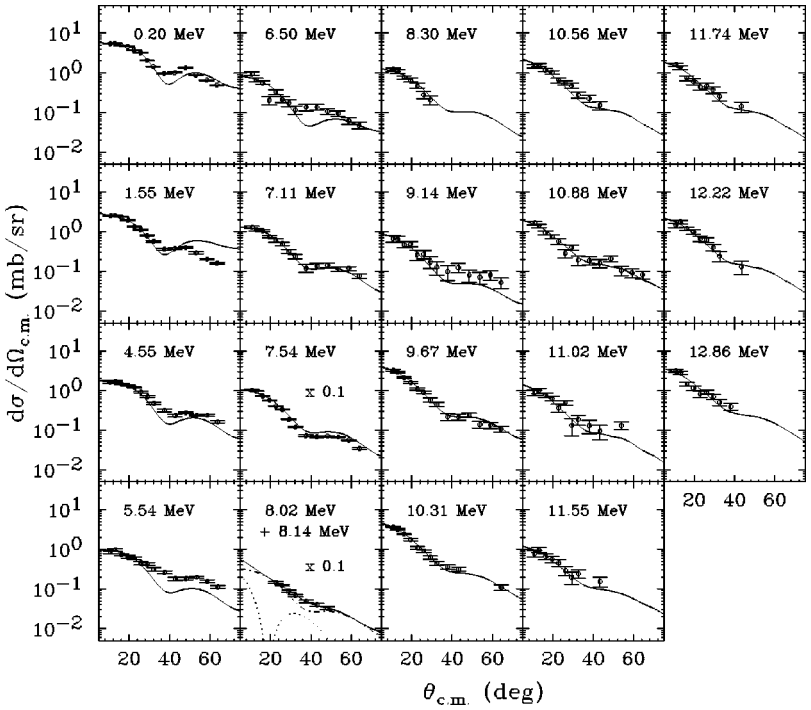

FIG. 3. Same as Fig. 2 but for the $l=2$ transitions. For experimentally unresolved transitions leading to the $E_{\rm exc}=8.02$-MeV and 8.14-MeV states, the solid line represents the result of the least-squares fit for the sum of theoretical $l=2$ (dot-dashed line) and 0 (dotted line) transitions to the data.

TABLE II. Experimental spectroscopic strengths in ^{19}F.

				$(2J+1)C^2S$			
E_{exc} (MeV) [a]	J^π; T [a]	E_{exc} (MeV) [b]	nlj [b]	[b]	[c]	[d]	[e]
0	$1/2^+$	0.00	$2s_{1/2}$	0.45	0.6	0.42	0.51
0.110	$1/2^-$				0.24	0.224	
0.197	$5/2^+$	0.20	$1d_{5/2}$	2.18	2.55	2.45	4.00
1.459	$3/2^-$				0.144	0.098	
1.554	$3/2^+$	1.55	$1d_{3/2}$	0.99	1.17	1.01	1.65
4.550	$5/2^+$	4.55	$1d_{5/2}$	0.39			
5.535	$5/2^+$	5.54	$1d_{5/2}$	0.18	0.29	0.31	0.44
6.088	$3/2^-$	6.09	$2p_{3/2}$	0.15	0.426	0.12	
6.255	$1/2^+$	6.26	$2s_{1/2}$	0.28	0.41	0.19	0.60
6.497	$3/2^+$	6.50	$1d_{3/2}$	0.13	0.133		0.24
6.787	$3/2^-$	6.79	$2p_{3/2}$	0.11	0.29	0.17	
6.927	$7/2^-$	6.93	$1f_{7/2}$	0.41		0.385	0.37
		7.11	$1d_{3/2}$, $1d_{5/2}$ [f]	0.21, 0.19 [f]	0.52	0.087	
7.540	$5/2^+$; 3/2	7.54	$1d_{5/2}$	1.33	0.82	0.665	1.76
8.014	$5/2^+$	8.06	$1d_{5/2}+2s_{1/2}$	0.38+0.22			0.40
8.138	$1/2^+$						
8.310	$5/2^+$	8.30	$1d_{5/2}$	0.14			
8.592	$3/2^-$	8.59	$2p_{3/2}$	0.15			
8.793	$1/2^+$; 3/2	8.79	$2s_{1/2}$	0.49			0.60
		9.14	$1d_{3/2}$ [f], $1d_{5/2}$	0.09 [f], 0.08			
9.668	$3/2^+$	9.67	$1d_{3/2}$	0.38			
10.308	$3/2^+$	10.31	$1d_{3/2}$	0.38			
10.555	$3/2^+$; (3/2)	10.56	$1d_{3/2}$	0.18			
10.86	$5/2^+$	10.88	$1d_{5/2}$	0.15			
		11.02	$1d_{3/2}$ [f], $1d_{5/2}$	0.11 [f], 0.10			
11.540	$5/2^+$	11.55	$1d_{5/2}$	0.11			
11.653	$3/2^+$; (3/2)	11.74	$1d_{3/2}$	0.18			
11.221	$3/2^+$	11.22	$1d_{3/2}$	0.25			
12.86	$3/2^+$;3/2	12.86	$1d_{3/2}$	0.48			
13.317	$7/2^-$; (3/2)	13.34	$1f_{7/2}$	0.22			0.11
13.732	$7/2^-$;3/2	13.75	$1f_{7/2}$	0.22			0.29

[a]Reference [18].
[b](d,n) reaction at 25 MeV (present work).
[c](^{3}He, d) reaction at 11 MeV (Ref. [11]).
[d](^{3}He, d) reaction at 16 MeV (Ref. [12]).
[e](α, t) reaction at 50 MeV (Ref. [13]).
[f]Assumed strength in sum-rule analysis.

model based on the complete space of $2s1d$ configurations. The shell-model wave functions for the $2s1d$-shell nuclei have been derived by Wildenthal [10] using an effective Hamiltonian specified by one-body and two-body matrix elements. The one-body matrix elements corresponding to single-particle energies were fixed for each $2s1d$-shell nucleus, while the mass dependence of $(18/A)^{0.3}$ was assumed for the two-body matrix elements between nucleon states. The Hamiltonian parameters have been fitted by a least-squares method to a set of about 440 energy data for $2s1d$-shell nuclei.

In order to interpret the proton single-particle strength in ^{19}F by means of the $2s1d$ shell model, one-particle parentage coefficients between the shell-model wave functions of $A=18$ and 19 systems were calculated with the code OXBASH [23].

IV. SPECTROSCOPIC RESULTS AND DISCUSSION

Spectroscopic results for the present experiment are summarized in Table II, together with the previous data [11–13]. Spins and parities J^π of the observed states in ^{19}F have already been assigned [24], except for those of the E_{exc} = 7.11-MeV, 9.14-MeV, and 11.02-MeV states. The experimental and theoretical strength distributions of the $2s1d$-shell orbitals are shown in Fig. 4.

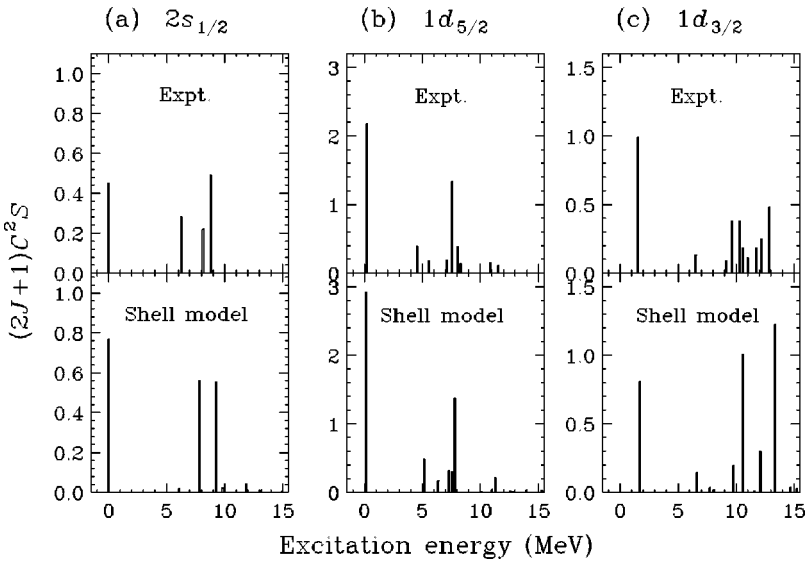

FIG. 4. Experimental and theoretical distributions (a) of the $2s_{1/2}$-proton strength, (b) of the $1d_{5/2}$-proton strength, and (c) of the $1d_{3/2}$-proton strength in ^{19}F. The experimental distributions are the results of the present study. The theoretical distributions are obtained from the shell-model calculation (Ref. [10]).

A. $l=0$ and 2 transitions

Large components of the $2s_{1/2}$ strength have been located at the $E_{\rm exc}=0$-MeV, 6.26-MeV, 8.14-MeV, and 8.79-MeV states. Figure 4(a) shows the experimental and theoretical distributions of the $2s_{1/2}$ proton strength. Significant strengths of the first $T=1/2$ and 3/2 states at $E_{\rm exc}=0$ and 8.79 MeV have been reproduced by the shell-model calculations [10]. A large theoretical strength predicted at $E_{\rm exc}=7.82$ MeV appears to be fragmented into two states at 6.26 and 8.14 MeV.

The $1d_{5/2}$ strength is concentrated in the lowest $T=1/2$ and 3/2 states at $E_{\rm exc}=0.20$ MeV and 7.45 MeV, respectively, while small strengths are distributed in the region $E_{\rm exc}=5-8$ MeV. The experimental results for the $1d_{5/2}$ strength have been properly reproduced by the shell-model estimate [10] as seen in Fig. 4(b).

In the case of the $1d_{3/2}$ orbital, a large amount of the strength, except for a dominant one at $E_{\rm exc}=1.55$ MeV, was missing in the previous proton-stripping experiments [11–13] although the shell model [10] predicts significant strengths in the high-lying region. The present work reveals many states with fragmented $1d_{3/2}$ strengths above $E_{\rm exc}=9$ MeV in addition to a low-lying dominant component at $E_{\rm exc}=1.55$ MeV. A comparison between the experimental result and the shell-model predictions [10] shown in Fig. 4(c) indicates that the shell model fails to reproduce the fragmentation of the high-lying strength, suggesting that more complex configurations including the $1p$-shell and/or $1f2p$-shell orbitals are needed for these states.

B. $l=1$ and 3 transitions

The $l=1$ transitions leading to the $3/2^-$ states at $E_{\rm exc}=6.09$, 6.79, and 8.59 MeV have been observed together with the $l=3$ transitions leading to the $7/2^-$ states at $E_{\rm exc}=6.93$, 13.32, and 13.73 MeV. The summations over the $1f_{7/2}$ and $2p_{3/2}$ strengths observed up to $E_{\rm exc}=14$ MeV correspond to about 11% and 10%, respectively, of the sum-rule limit.

C. Summed strengths and centroid energies

Summed spectroscopic strengths of the $2s1d$ orbitals and their centroid energies are compared with the shell-model predictions [10] in Table III. The errors show only the statistical errors resulting from the least-squares fits of the theoretical cross sections to the data. For the $l=2$ transitions into unknown J^π states at $E_{\rm exc}=7.11$, 9.14, and 11.02 MeV, assumed spins ($J=3/2$ or 5/2) are indicated in Table II.

The present analysis shows that most of the $2s1d$ strengths have been located below $E_{\rm exc}=14$ MeV. This observation appears to be supported by the shell-model calculation [10]. The centroid energies of the $1d_{5/2}$ and $2s_{1/2}$

TABLE III. Sums of the single-particle strengths in ^{19}F and their centroid energies.

	$\Sigma(2J+1)C^2S$			Centroid energy (MeV)		
Orbital	Experiment	Calculations (Ref. [10])		Experiment	Calculations (Ref. [10])	
nlj	a	a	b	a	a	b
$1d_{5/2}$	5.05±0.41	5.90	6	4.30±0.30	3.91	4.14
$2s_{1/2}$	1.44±0.82	1.98	2	5.45±1.61	5.31	5.45
$1d_{3/2}$	3.17±0.30	3.75	4	7.97±0.46	9.46	9.90

[a]Evaluated for final states up to $E_{\rm exc}=14$ MeV.
[b]Evaluated for all final states.

TABLE IV. Occupation probabilities O_{lj} and single-particle energies E_{lj} of the proton orbitals in ^{18}O.

Orbital nlj	O_{lj}		E_{lj} (MeV)	
	Experiment	Calculations (Ref. [10])	Experiment	Calculations (Ref. [10])
$1p_{1/2}$	0.87 ± 0.07	1	-14.95 ± 0.42	
$2s_{1/2}$	0.19 ± 0.02	0	-5.31 ± 0.49	-2.54
$1d_{5/2}$	0.07 ± 0.02	0	-4.81 ± 0.23	-3.85

strengths in the probed region are in good agreement with the theoretical values, while the predicted energy for the $1d_{3/2}$ strength is higher than the observed value by about 1.5 MeV.

D. Occupation probabilities and single-particle energies

Occupation probabilities and single-particle energies of proton orbitals near the Fermi surface for ^{18}O have been estimated according to the procedure used in the previous studies [5–7]. This method is based on a relation between the single-particle strengths obtained from stripping and those from pickup reactions on the same target:

$$\sum G_{lj}^{+}+\sum G_{lj}^{-}=2j+1, \tag{2}$$

where $+$ and $-$ denote values for stripping and pickup reactions, respectively, and

$$G_{lj}^{+}=(2j+1)C^2S_{lj}, \tag{3}$$

$$G_{lj}^{-}=C^2S_{lj}. \tag{4}$$

Evaluation of the occupation probability needs the summation of the strengths over all final states. However, it is experimentally difficult to measure the high-lying strengths in the continuum region. Furthermore, the summation of the strengths may be inaccurate since absolute spectroscopic factors strongly depend on distorted-wave Born approximation parameters. Thus, one makes two assumptions in this method. First, relative spectroscopic factors can be extracted with high precision. Second, the summations of observed strengths for individual orbitals near the Fermi surface correspond to the same fraction of the total strengths for the respective orbitals. Under these assumptions one may rewrite Eq. (2) as follows:

$$n^{+}\sum G_{lj}^{+}+n^{-}\sum G_{lj}^{-}=2j+1, \tag{5}$$

where n^{+} and n^{-} are normalization factors which are determined from the linear regression so that Eq. (5) is simultaneously satisfied for the individual orbitals. Using these normalization factors we define the occupation probability as an average of the results for the stripping and pickup reactions:

$$O_{lj}=\frac{1}{2}\left[\left(1-\frac{n^{+}\sum G_{lj}^{+}}{2j+1}\right)+\left(\frac{n^{-}\sum G_{lj}^{-}}{2j+1}\right)\right]. \tag{6}$$

According to Baranger's definition [25] a single-particle energy is given as a centroid energy evaluated from both the stripping and pickup strengths:

$$E_{lj}=\frac{E_{lj}^{+}n^{+}\sum G_{lj}^{+}+E_{lj}^{-}n^{-}\sum G_{lj}^{-}}{n^{+}\sum G_{lj}^{+}+n^{-}\sum G_{lj}^{-}}, \tag{7}$$

where

$$E_{lj}^{+}=\frac{\sum G_{lj}^{+}E_{\mathrm{exc}}^{+}}{\sum G_{lj}^{+}}-B(A+1), \tag{8}$$

$$E_{lj}^{-}=-\frac{\sum G_{lj}^{-}E_{\mathrm{exc}}^{-}}{\sum G_{lj}^{-}}-B(A). \tag{9}$$

Here, $B(A)$ denotes the one-proton separation energy in the ground state of a nucleus with mass A.

In the present work we deal with the proton $1p_{1/2}$, $2s_{1/2}$, and $1d_{3/2}$ orbitals of ^{18}O. The stripping data were taken from the present results for the $2s1d$ orbitals, and from the (^{3}He, d) result [12] for the $1p_{1/2}$ orbital. The pickup data were taken from the (d,^{3}He) result [14]. Occupation probabilities and single-particle energies obtained from the analysis are listed in Table IV. The resulting normalization factors were $n^{+}=1.10\pm0.03$ and $n^{-}=0.86\pm0.15$. The uncertainties were estimated from the statistical errors. The result for the analysis indicates that the occupation probabilities deviate from expectation of a simple shell model that predicts proton shell closure up to the $1p_{1/2}$ orbital, in other words, the empty $2s1d$ shell for oxygen isotopes. These deviations are probably due to configuration mixing caused by ground-state correlations. As seen from Table IV, the shell model [10] employed in the present work does not account for the experimental results, since the calculations included only $2s1d$-shell orbitals. The explanation of the experimental results seems to require shell-model calculations including the $1p$-shell as well as $2s1d$-shell orbitals.

V. SUMMARY AND CONCLUSION

The distributions of the proton single-particle strengths in ^{19}F up to $E_{\mathrm{exc}}=14$ MeV have been deduced via the

^{18}O(d,n) reaction at 25 MeV. Almost all the $1d_{5/2}$ and $2s_{1/2}$ strengths have been observed in the present measurement. Many states with fragmented $1d_{3/2}$ strengths have newly been identified above $E_{\rm exc}=9$ MeV in the present measurement. The observed $1d_{3/2}$ strengths amount to about 80% of the shell-model limit.

The results of the present measurement were compared with the shell-model predictions [10] with the complete $2s1d$ configurations. The strength distributions and their centroid energies for the $1d_{5/2}$ and $2s_{1/2}$ protons are in good agreement with the shell model. On the other hand, the theoretical results for the $1d_{3/2}$ proton are unsatisfactory. In particular, the shell-model calculations have failed to reproduce the fragmentation of the high-lying $1d_{3/2}$ components. The present work suggests that more complex configurations are needed to explain high-lying $3/2^+$ states.

We deduced occupation probabilities and single-particle energies of the $1p_{1/2}$, $1d_{5/2}$ and $2s_{1/2}$ proton orbitals in the ground state of ^{18}O. Obtained occupation probabilities deviate from the simple shell-model values.

ACKNOWLEDGMENTS

The authors acknowledge the SUMITOMO cyclotron staff at CYRIC for their help during the present experiment. Thanks are due to M. Kato for assistance in preparing the gas cell, and Professor K. Muto for useful discussions. One of the authors (H.Oh.) acknowledges partial financial support by The Ministry of Education, Science, Sports and Culture under a Grant-in-Aid for Scientific Research (C) Grant No. 09640371.

[1] M. H. Macfarlane and J. B. French, Rev. Mod. Phys. **32**, 567 (1960).
[2] J. B. French and M. H. Macfarlane, Nucl. Phys. **26**, 168 (1966).
[3] P. Grabmayr, Prog. Part. Nucl. Phys. **29**, 251 (1992).
[4] P. Grabmayr, A. Mondry, G. J. Wagner, P. Woldt, G. P. A. Berg, J. Lisantti, D. W. Miller, H. Nann, and E. J. Stephenson, Phys. Rev. C **49**, 2971 (1994).
[5] A. Pfeiffer, G. Mairle, K. T. Knöpfle, T. Kihm, G. Seegert, P. Grabmayr, G. J. Wagner, V. Bechtold, and L. Fgriedrich, Nucl. Phys. **A455**, 381 (1986).
[6] S. Khan, G. Mairle, K. T. Knöpfle, Th. Kihm, Liu-Ken Pao, P. Grabmayr, G. J. Wagner, and L. Friedlich, Nucl. Phys. **A481**, 253 (1988).
[7] G. Mairle, M. Seeger, H. Reinhardt, T. Kihm, K. T. Knöpfle, and Chen Lin Wen, Nucl. Phys. **A565**, 543 (1993).
[8] K. Miura, T. Tohei, T. Nakagawa, A. Sato, T. Ishimatsu, T. Kawamura, K. Furukawa, M. Kabasawa, Y. Takahashi, H. Orihara, T. Niizeki, K. Ishii, and H. Ohnuma, Nucl. Phys. **A467**, 79 (1987).
[9] A. Terakawa, T. Tohei, T. Nakagawa, A. Sato, J. Takamatsu, M. Mori, A. Narita, H. Orihara, K. Ishii, T. Niizeki, M. Oura, S. Hirasaki, M. Hosaka, G. C. Jon, K. Miura, and H. Ohnuma, Phys. Rev. C **48**, 2775 (1993).
[10] B. H. Wildenthal, Prog. Part. Nucl. Phys. **11**, 5 (1984).
[11] L. L. Green, C. O. Lennon, and J. M. Naqib, Nucl. Phys. **A142**, 137 (1970).
[12] C. Schmidt and H. H. Duhm, Nucl. Phys. **A155**, 644 (1970).
[13] M. Yasue, T. Hasagawa, S. I. Hayakawa, K. Ieki, J. Kasagi, S. Kubono, T. Murakami, K. Nisimura, K. Ogawa, H. Ohnuma, R. J. Peterson, H. Shimizu, M. H. Tanaka, and H. Toyokawa, Phys. Rev. C **46**, 1242 (1992).
[14] G. Mairle, K. T. Knöpfle, P. Doll, H. Breuer, and G. J. Wagner, Nucl. Phys. **A280**, 97 (1977).
[15] H. Orihara and T. Murakami, Nucl. Instrum. Methods **181**, 15 (1981).
[16] H. Orihara, S. Nishihara, K. Furukawa, M. Kabasawa, T. Kawamura, Y. Takahashi, T. Nakagawa, and K. Maeda, Nucl. Instrum. Methods Phys. Res. A **257**, 189 (1987).
[17] P. D. Kunz, computer code DWUCK.
[18] R. C. Johnson and P. J. R. Sorper, Phys. Rev. C **1**, 976 (1970).
[19] G. L. Wales and R. C. Johnson, Nucl. Phys. **A274**, 168 (1976).
[20] F. D. Becchetti and G. W. Greenlees, Phys. Rev. **182**, 1190 (1969).
[21] Ph. Martin, Nucl. Phys. **A466**, 119 (1987).
[22] C. M. Vincent and H. T. Fortune, Phys. Rev. C **2**, 782 (1970).
[23] A. Etchegoen, W. D. M. Rae, and N. S. Godwin, shell-model code OXBASH82, and extended as MSU version by B. A. Brown, W. E. Ormand, and J. S. Winfield.
[24] D. R. Tilly, H. R. Wellller, C. M. Cheves, and R. M. Chasteler, Nucl. Phys. **A595**, 1 (1995).
[25] M. Baranger, Nucl. Phys. **A149**, 225 (1970).